Asian Journal of Chemistry; Vol. 27, No. 7 (2015), 2359-2364

ASIAN JOURNAL OF CHEMISTRY

http://dx.doi.org/10.14233/ajchem.2015.17829

Magnetic, Photophysical and Thermal Properties of Complexes of Iron(II) with Structurally Different Schiff Bases

NORBANI ABDULLAH*, AFIQ AZIL, ANITA MARLINA and NUR LINAHAFIZZA M. NOOR

Department of Chemistry, Faculty of Science, University of Malaya, 50603 Kuala Lumpur, Malaysia

*Corresponding author: Fax: +60 3 79674193; Tel: +60 3 79674264; E-mail: norbania@um.edu.my, anitamarlina@siswa.um.edu.my

Received: 16 April 2014; *Accepted*: 30 May 2014; *Published online*: 30 March 2015; AJC-17033

Three Fe(II) complexes of structurally different Schiff bases *i.e.*, $[Fe(L1)_2](BF_4)$ (**1**), $[Fe_2(OOC(CH_2)_{14}CH_3)_2(L_2)(H_2O)_2]$ (**2**) and $[Fe_2(OOC(CH_2)_{14}CH_3)_2(L_3)(H_2O)_4]\cdot 2.5H_2O$ (**3**), were synthesized and characterised for potential uses as spin crossover and low band gap materials with metallomesogenic properties. Complex **1** was obtained in a one-pot reaction involving $Fe(BF_4)_2$ with L1, while compounds **2** and **3** were obtained by step-wise reactions involving $[Fe(OOC(CH_2)_{14}CH_3)_2(EtOH)]$ with H_2L2 and H_2L3, respectively. At room temperature, compound **1** has a low-spin Fe(II) atom while both compounds **2** and **3** have two high-spin Fe(II) atoms. The values for the optical band gap (E_g) were 1.8 eV for compound **1**, 1.9 eV for compound **2** and 2.3 eV for compound **3**. These complexes were thermally stable, with decomposition temperature of 260 °C for compound **1**, 205 °C for compound **2** and 250 °C for compound **3**. Complexes **1** and **2** exhibited mesomorphisms while **3** was not mesomorphic.

Keywords: Iron(II), Schiff base, Spin crossover, Bandgap, Metallomesogen.

INTRODUCTION

Fe(II) complexes made up of N-donor ligands are widely investigated as spin crossover (SCO) materials. This is because the valence electronic configuration of Fe(II) ($3d^6$) may be reversibly switched between low spin (LS, t_{2g}^6) and high spin (HS, $t_{2g}^4e_g^2$) state by external stimuli, such as temperature, pressure and light irradiation[1-6]. More recently, Fe(II) complexes are attracting attention as potential photosensitizers in dye-sensitized solar cells (DSSC)[7-9], to replace the more expensive and toxic Ru(II) complexes[10-15]. For these purposes, ligands derived from Schiff bases are ideally suited as they are easy to prepare, structurally versatile and form stable complexes with most transition metal ions[16-19].

This paper presents the syntheses of three structurally different Schiff bases, L1, H_2L2 and H_2L3 (Fig. 1) and the corresponding Fe(II) complexes. Ligand L1 was a neutral N_3-donor Schiff base, H_2L2 was a multi-N donor conjugated Schiff base and H_2L3 has two N,O-donors separated by an eight-carbon aliphatic chain. The main objective was to show the effect of different donor atoms of the ligands on the structures, magnetic, photophysical and thermal properties of Fe(II) complexes formed. $[Fe(L1)_2](BF_4)_2$ (**1**) was formed in a one-pot reaction involving $Fe(BF_4)_2\cdot 6H_2O$ and L1, while $[Fe_2(OOC(CH_2)_{14}CH_3)_2(L_2)(H_2O)_2]$ (**2**) and $[Fe_2(OOC(CH_2)_{14}CH_3)_2(L_3)(H_2O)_4]\cdot 2½H_2O$ (**3**) were formed in step-wise reactions involving $[Fe(OOC(CH_2)_{14}CH_3)_2(EtOH)]$ with H_2L2 and H_2L3, respectively. A common feature of these complexes was the presence of linear 16-carbon alkyl chains, introduced in order to lower their melting temperatures[20] and to induce mesomorphism (s)[21,22].

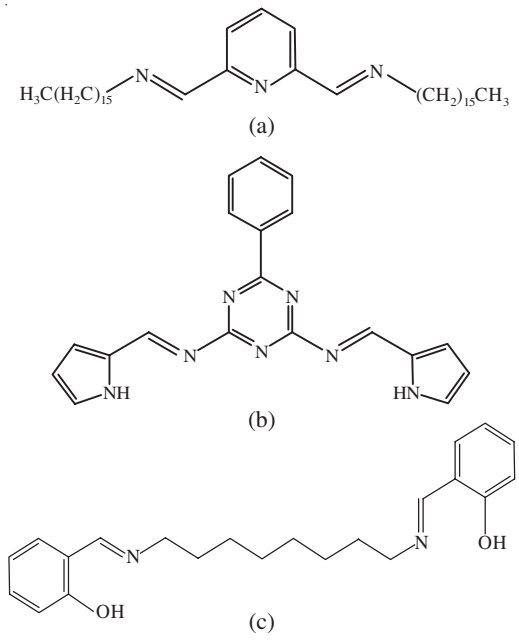

Fig. 1. Structural formulae of Schiff bases: (a) L1; (b) H_2L2; and (c) H_2L3

EXPERIMENTAL

All chemicals were analaR reagents and used as received. The elemental analyses (CHN) were carried out on a Thermo Finnigan Flash EA 1112. The ^{1}H NMR spectra were recorded in $CDCl_3$ and DMSO on a JEOL FT-NMR lambda 400 MHz spectrometer. The FTIR spectra were recorded for neat samples from 4000 to 450 cm^{-1} on a Perkin-Elmer Frontier FTIR spectrometer equipped with a diamond attenuated total reflectance attachment. Magnetic susceptibility at room temperature was determined on a Sherwood automagnetic susceptibility balance by the Gouy method. The instrument was calibrated using $Hg[Co(NCS)_4]$ and the molar susceptibility value was corrected for the diamagnetism of the constituent atoms using Pascal's constants. Variable temperature magnetic susceptibility was measured on a Quantum Design MPMS XL EverCool SQUID magnetometer at Kinki University, Higashiosaka-shi, Osaka, Japan. About 10 mg of the sample was placed inside a gelatine capsule and inserted halfway inside a drinking straw to a depth of about 10 cm from the top. The straw was then inserted into the instrument. The measurements were recorded at 1 Tesla (10,000 Gauss) in the temperature range of 300-4 K. The raw data was analysed using Microsoft Excel and IGOR Pro. The UV-visible spectrum was recorded in $CHCl_3$ and DMSO from 1200 to 400 nm on a Shimadzu UV-visible-NIR 3600 spectrophotometer. Thermogravimetric analysis (TGA) was done on a Perkin-Elmer Pyris Diamond TG/DTA thermal instrument under N_2 at a flow rate of 10 cm^3 min^{-1}. The temperature range was 50-900 °C and the scan rate was 20 °C min^{-1}. Differential scanning calorimetry (DSC) was done on a Mettler Toledo DSC 822 calorimeter in the temperature range 25 °C to a maximum 250 °C under N_2 at a flow rate of 20 cm^3 min^{-1} and a scan rate of 10 °C min^{-1}. The scans were recorded during one heating-and-cooling cycle for all complexes and the onset temperatures were quoted for all peaks observed. Polarising optical microscopy (POM) was carried out on an olympus polarizing microscope equipped with a Mettler Toledo FP90 central processor and a Linkam THMS 600 hot stage. The sample was heated in an oven at 60 °C for a few days prior to the analysis. The heating and cooling rates were 10 and 3 °C min^{-1}, respectively and the magnification was 50x.

Syntheses

$[Fe(L1)_2](BF_4)_2$ (1): $Fe(BF_4)_2{\cdot}6H_2O$ (0.34 g, 1.01 mmol) was added portionwise to a magnetically stirred methanolic solution (25 mL) of 2,6-pyridinedicarboxaldehyde (0.28 g, 2.07 mmol) and 1-aminohexadecane (0.97 g, 4.05 mmol) at room temperature. The mixture was further stirred at room temperature for 1 h. The purplish black powder obtained was filtered and washed with diethyl ether. Yield: 1.1 g (77.2 %). Anal. Calcd. for $C_{78}H_{142}N_6B_2FeF_8$ (1393.5 g mol^{-1}): C, 67.2; H, 10.3; N, 6 %. Found: C, 67.1; H, 11.4; N, 5.9 %.

$[Fe(OOC(CH_2)_{14}CH_3)_2(EtOH)]$: $FeSO_4{\cdot}7H_2O$ (5.10 g, 18.3 mmol) was added to a hot ethanolic solution (50 mL) of $CH_3(CH_2)_{14}COONa$ (10.23 g, 36.7 mmol). The mixture was heated for 0.5 h and the fine light brown powder formed was filtered under suction, washed with distilled water followed by ethanol and then dried in an oven at 60 °C. Yield: 8.3 g (73.7 %). Anal. Calcd. for $C_{34}H_{68}O_5Fe$ (612.8 g mol^{-1}): C, 66.6; H, 11.2 %. Found: C, 66.4; H, 12.5 %.

H_2L2: An ethanolic mixture (30 mL) of pyrrole-2-carboxaldehyde (11.69 g, 123 mmol) and 2,4-diamino-6-phenyl-1,3,5-triazine (11.52 g, 61.5 mmol) was refluxed for 3 h in the presence of a few drops of glacial acetic acid. A brownish powder obtained was filtered from the hot reaction mixture, washed with ethanol and dried in an oven at 100 °C. Yield: 15.8 g (68.3 %). Anal. Calcd. for $C_{19}H_{15}N_7$ (341.4 g mol^{-1}): C, 66.9; H, 4.4; N, 28.7 %; found: C, 66.9; H, 4.9; N, 29 %. ^{1}H NMR (DMSO-d_6): 6.75 (d, 4H), 7.43-7.49 (d, 3H), (7.51 (s, 2H), 8.23 (d, 2H), 8.25 (d, 2H), 11.3 (s, 2H).

$[Fe_2(OOC(CH_2)_{14}CH_3)_2(L_2)(H_2O)_2]$ (2): $[Fe(OOC(CH_2)_{14}CH_3)_2(EtOH)]$ (0.15 g, 0.24 mmol) was added to an ethanolic suspension (25 mL) of H_2L2 (0.09 g, 0.26 mmol) and the reaction mixture was refluxed for 3 h. The pale brown powder formed was filtered from the hot reaction mixture, washed with ethanol and dried in an oven at 100 °C. Yield: 0.21 g (87.7 %). Anal. Calcd. for $C_{51}H_{79}N_7O_6Fe_2$ (997.9 g mol^{-1}): C, 61.4; H, 7.9; N, 9.8 %; found: C, 61.2; H, 7.6; N, 9.1 %.

H_2L3: 2-Hydroxybenzaldehyde (4.88 g, 40 mmol) was added to an ethanolic solution (100 mL) of 1,8-diaminooctane (2.89 g, 20 mmol) and the reaction mixture was refluxed for 3 h in the presence of a few drops of glacial acetic acid. The yellow crystalline solid obtained from the cooled reaction mixture was filtered, washed with ethanol and left to dry at room temperature. Yield: 5.37 g (76.1 %). ^{1}H NMR ($CDCl_3$): 1.2-1.7 (m, 4H), 3.5 (t, 1H), 6.8 (t, 1H), 6.9 (d, 1H), 7.2 (t, 1H), 7.3 (d, 1H), 8.3 (s, 1H), 13.6 (s, 1H). Anal. Calcd. for $C_{22}H_{28}N_2O_2$ (352.5 g mol^{-1}): C, 75; H, 8; N, 8 %; found: C, 75.3; H, 7.9; N, 8.2 %.

$[Fe_2(OOC(CH_2)_{14}CH_3)_2(L3)(H_2O)_4]{\cdot}2.5H_2O$ (3): $[Fe(OOC(CH_2)_{14}CH_3)_2(EtOH)]$ (0.42 g, 0.69 mmol) and H_2L3 (0.27 g, 0. 76 mmol) were refluxed in ethanol (100 mL) for 3 h. The brown powder formed was filtered and dried at room temperature. Yield: 0.35 g (46.6 %). Anal. Calcd. for $C_{54}H_{101}N_2O_{12.5}Fe_2$ (1090 g mol^{-1}): C, 59.4; H, 9.3; N, 2.6 %. Found: C, 59.1; H, 8.8; N, 2.9 %.

RESULTS AND DISCUSSION

Syntheses and structural elucidation: Complex **1** ($[Fe(L1)_2](BF_4)_2$) was obtained as a dark purple powder in high yield from a one-pot reaction involving 2,6-pyridinedicarboxaldehye, 1-aminohexadecane and iron(II) tetrafluroborate hexahydrate (mole ratio 2:4:1, **Scheme-I**). It was soluble in methanol, ethanol, dichoromethane and chloroform. Its chemical formula was supported by CHN elemental analyses and by IR spectroscopy discussed below.

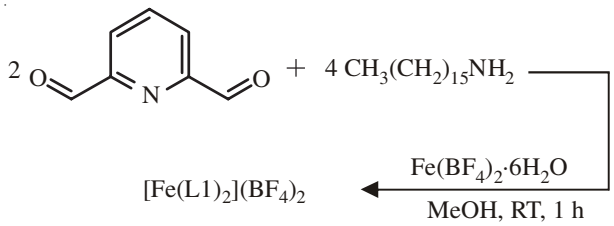

Scheme-I: Equation for the preparation of compound **1**

Its IR spectrum showed two strong peaks at 2916 and 2850 cm^{-1} for $\nu_{asym}CH_2$ and $\nu_{sym}CH_2$, respectively, a weak peak at 1636 cm^{-1} for νC=N, a strong peak at 1024 cm^{-1} for νB-F of noncoordinated BF_4^- ion[23] and a medium peak at 519 cm^{-1} for νFe-N. From these, it may be inferred that L1 was coordinated to Fe(II) ion as a neutral N_3-donor ligand (Fig. 2).

In contrast, complexes **2** ($Fe_2(OOC(CH_2)_{14}CH_3)_2(L2)(H_2O)_2$]) and **3** ([$Fe_2(OOC(CH_2)_{14}CH_3)_2$ $(L3)(H_2O)_4$]·$2.5H_2O$) were obtained in high yields in step-wise reactions involving [$Fe(OOC(CH_2)_{14}CH_3)_2(EtOH)$] and H_2L_2 and H_2L_3, respectively (**Scheme-II**). Both complexes were dinuclear with octahedral Fe(II) centres. Complex **2** was soluble in DMSO and THF, while complex **3** was soluble in chloroform and dichloromethane. As for compound **1**, the chemical formulae for compounds **2** and **3** were supported by CHN elemental analyses and IR spectroscopy.

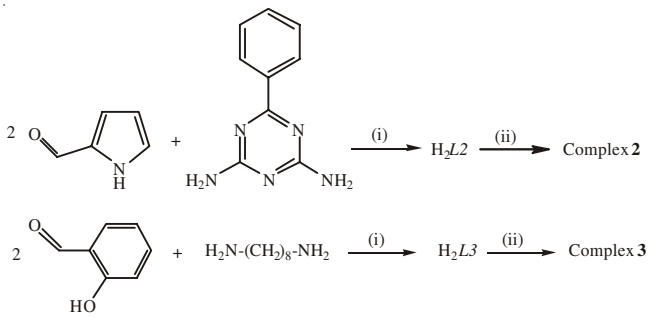

Scheme-II: Equations for the preparation of compounds **2** and **3**: (i) EtOH, HOAc, 3 h reflux; (ii) [$Fe(OOC(CH_2)_{14}CH_3)(EtOH)$], EtOH, 3 h reflux

The IR spectrum of compound **2** showed two broad peaks centred at 3333 and 3138 cm^{-1} for H-bonded H_2O molecules, two strong peaks at 2918 and 2850 cm^{-1} for $\nu_{asym}CH_2$ and $\nu_{sym}CH_2$, respectively, a strong peak at 1618 cm^{-1} for ν(C=N), a strong peak at 1530 cm^{-1} for $\nu_{asym}COO$, a strong peak at 1393 cm^{-1} for $_{sym}COO$, a weak peak at 578 cm^{-1} for ν(Fe-N) and a weak peak at 491 cm^{-1} for ν(Fe-O)[24]. For comparison, the IR spectrum of H_2L2 showed a weak peak at 3295 cm^{-1} for ν(N-H) and a strong peak at 1615 cm^{-1} for ν(C=N). Hence, it may be inferred that in the formation of compound **2**, H_2L_2 were doubly deprotonated at pyrrole N-H, the iminyl nitrogen atoms were not involved in the bonding and the binding mode of $CH_3(CH_2)_{14}COO^-$ ion to Fe(II) atoms was bidentate chelating (Δ = 137 cm^{-1})[25] (Fig. 2).

The IR spectrum of compound **3** showed a weak peak at 3396 cm^{-1} for water, two strong peaks at 2917 and 2849 cm^{-1} for $\nu_{asym}CH_2$ and $\nu_{sym}CH_2$, respectively, a weak peak at 1612 cm^{-1} for νC=N, a strong peak at 1574 cm^{-1} for $\nu_{asym}COO$, a strong peak at 1446 cm^{-1} for $\nu_{sym}COO$, a medium peak at 592 cm^{-1} for νFe-N and a medium peak at 461 cm^{-1} for ν(Fe-O)[24]. For comparison, the IR spectrum of H_2L3 showed a weak peak at 3406 cm^{-1} for ν(O-H), two strong peaks at 2919 cm^{-1} and 2851 cm^{-1} for $\nu_{asym}CH_2$ and $\nu_{sym}CH_2$, respectively and a strong peak at 1633 cm^{-1} for ν(C=N). Hence, it may be inferred that in the formation of compound **3**, the two phenolic O-H group of H_2L3 was deprotonated and the phenolic oxygen and iminyl nitrogen were coordinated to Fe(II) atom. In addition, the Δ value for $CH_3(CH_2)_{14}COO^-$ ligand was 128 cm^{-1}, suggesting a chelating binding mode to both Fe(II) centres[25] (Fig. 2).

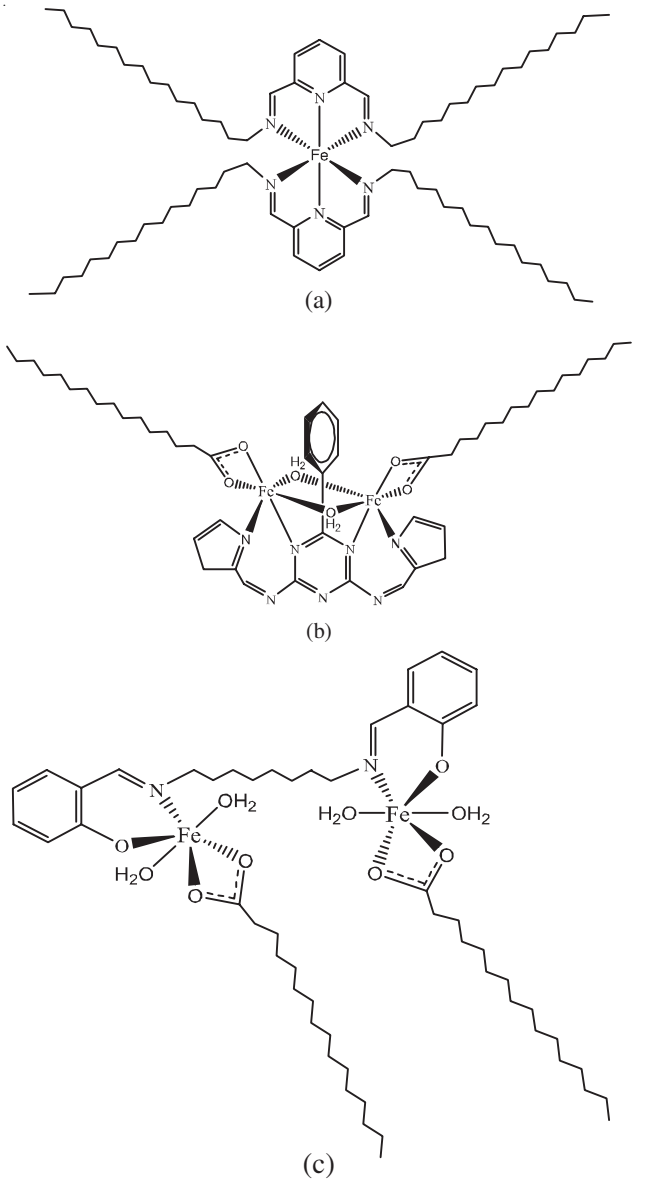

Fig. 2. Proposed structures of: (a) compound **1** ($(BF_4)_2$); (b) compound **2**; and (c) compound $3{\cdot}2.5H_2O$

Magnetic and photophysical properties: Complex **1** was diamagnetic at room temperature as the value of its mass susceptibility (χ_g), determined by the Gouy method, was negative. Its electronic absorption spectrum in chloroform shows two strong intraligand bands at 473 nm (ε_{max} = 6476 M^{-1} cm^{-1}) and 576 nm (ε_{max} = 7100 M^{-1} cm^{-1}), a strong singlet metal-to-ligand charge transfer band (^{1}MLCT) at 596 nm (ε_{max} = 8710 M^{-1} cm^{-1}) assigned to $t_{2g} \rightarrow \pi^*$ electronic transition[9] and a weaker *d-d* band at 721 nm (ε_{max} = 470 M^{-1} cm^{-1}) assigned to $^1A_{1g} \rightarrow {}^1T_{1g}$ electronic transition[26]. Hence, compound **1** was a low-spin iron(II) complex. From this, it may be inferred that L1 was a strong field ligand. From the electronic spectral data, the optical band gap (E_g) for compound **1**, calculated using the equation: $E_g = hc/\lambda$, where c = velocity of light, h = Planck constant and λ (absorption edge of CT band) = 688 nm)[27], was 1.8 eV.

In contrast, compound **2** was paramagnetic at room temperature. The value of $\chi_M T$ (χ_M = molar magnetic susceptibility and T = temperature in K), as determined by the Gouy method,

was 6.2 cm^3 K mol^{-1} at 298 K. The expected value for a dimeric high spin Fe(II) octahedral complex[28] is 6 cm^3 K mol^{-1}. From these, it may be inferred that both Fe(II) atoms in the complex were high spin, with negligible electronic communication between the two Fe(II) centres. Thus, $L2^{2-}$ ion was a weak field ligand. The electronic absorption spectrum for the complex in DMSO shows a shoulder at 488 nm (ε_{max} = 3478 M^{-1} cm^{-1}) assigned to the intraligand electronic transition and a weak d-d band at 773 nm (ε_{max} = 489 M^{-1} cm^{-1}) assigned to $^5T_{2g} \rightarrow {}^5E_g$ electronic transition[29,30]. The E_g value, similarly calculated as for compound **1** using λ = 630 nm, was 1.9 eV.

For compound **3**, the value of $\chi_M T$, as determined by the Gouy method, was 4.17 cm^3 K mol^{-1} at 300 K. Since low spin Fe(II) is diamagnetic (t_{2g}^6) and the expected $\chi_M T$ value for a complex with two high spin Fe(II) atoms and g = 1.3 (see below)[29] is 2.54 cm^3 K mol^{-1}, it may be inferred that compound **3** comprised of two high spin Fe(II) atoms at this temperature[31]. Additionally for compound **3**, its temperature-dependence magnetic susceptibility was measured using a SQUID magnetometer in the temperature range 300-2 K. The experimental curve of $\chi_M T$ versus T (Fig. 3) shows a good fit with the theoretical curve constructed from the formula for a symmetrical dinuclear complex given below[28] and inserting the values of g = 1.3 and J (the isotropic interaction parameter) = -28.4 cm^{-1} into the formulae:

$$\chi_m = \frac{Ng^2\beta^2\Sigma_s S(S+1)\exp\left[-\frac{E(S)}{kT}\right]}{\Sigma_S(2S+1)\exp\left[-\frac{S}{kT}\right]}$$

$$E(S) = -\frac{J}{2}S(S+1)$$

From Fig. 3, it is noted that the $\chi_M T$ values decreased gradually from 4.15 cm^3 K mol^{-1} at 294 K to 2.03 cm^3 K mol^{-1} at 8.8 K and then more rapidly to about 1.78 cm^3 K mol^{-1} at 4 K as a result of zero-field splitting. It is also noted that the g value for compound **3** was significantly lower than the theoretical value (2.0023), suggesting a highly distorted octahedral environment, expected for high spin Fe(II) atoms due to the weak Fe-L bonds. The low J value (-28.4 cm^{-1}) indicates a weak antiferromagnetic interaction between the two Fe(II) centres, postulated to occur through H-bonds between the coordinated and lattice H_2O[32]. The results suggest a normal but incomplete SCO behaviour in this temperature range.

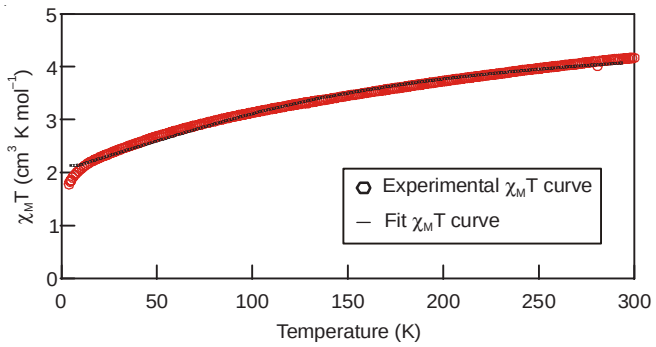

Fig. 3. Plot of $\chi_M T$ *vs.* T for compound **3**

The electronic absorption spectrum of compound **3** in chloroform shows two overlapping bands at 468 nm (ε_{max} = 114.3 M^{-1} cm^{-1}) and 510 nm (ε_{max} = 63.5 M^{-1} cm^{-1}) assigned to intraligand electronic transitions. The E_g value was 2.3 eV (λ_{onset} = 534 nm).

Thermal properties: The thermal data (TGA and DSC) for complexes **1-3** are shown in Table-1. The TGA traces are shown in Fig. 4, while the DSC scans are shown in Fig. 5.

TABLE-1
THERMAL DATA FOR COMPLEXES **1-3**

Complex	TGA T_{dec} (°C)	DSC T_{onset}/°C (ΔH/kJ mol^{-1})					
		Heating			Cooling		
1	260	62.6 (+16.0)	89.6 (+94.1)	–	44.5 (–54.1)	–	–
2	205	56.4 (–11.7)	85.3 (+64.2)	176.8 (+55.6)	166. (.31.8	57.6 –21.9	40.6 (–28.6
3	250	77* (+48.7)	–	–	–	–	–

* Two overlapping endotherms

The TGA trace for compound **1** (Fig. 4a) shows a gradual weight loss totaling 90.2 % on heating from 260 °C to about 640 °C. This may be due to the decomposition of BF_4^- ion and L1 ligand (expected 93.3 %). The amount of residue above this temperature was 9.8 %. For compound **2**, the TGA trace (Fig. 4b) shows a rapid weight loss of 90.4 % on heating from about 205 to 620 °C. This may be due to evaporation of coordinated H_2O and decomposition of $CH_3(CH_2)_{14}COO^-$ and L2 ligands (expected 88.8 %). The amount of residue above this temperature was 9.6 %. For compound **3**, the TGA trace (Fig. 4c) shows an initial weight loss of 4.1 % in the temperature range 100-250 °C, assigned to evaporation of lattice H_2O (expected 3.5 %). On further heating to about 660 °C, it suffered a total weight loss of 78 %, assigned to loss of coordinated H_2O and decomposition of $CH_3(CH_2)_{14}COO^-$ (expected 85.1 %). The amount of residue above this temperature was 17.9 %.

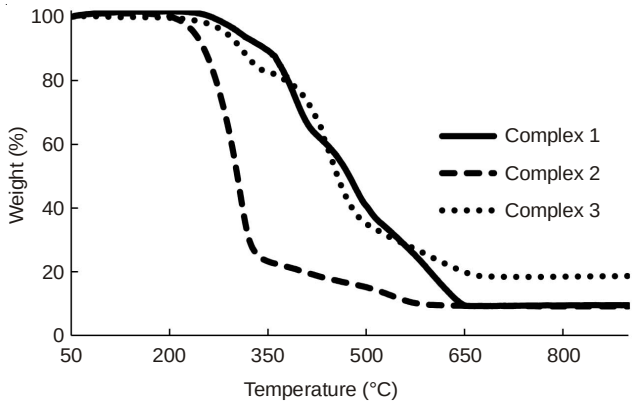

Fig. 4. TGA traces of (a) compound **1**; (b) compound **2**; and (c) compound **3**

For phase transitions, the DSC of complex **1** (Fig. 5a) shows two endotherms on heating at 62.6 °C (ΔH = +16.0 kJ mol^{-1}) assigned to crystal-to-crystal transition and at 89.6 °C (ΔH = +94.1 kJ mol^{-1}) assigned to crystal-to-mesophase transition. On cooling from 150 °C, there was an exotherm at 44.5 °C (ΔH = -54.1 kJ mol^{-1}) assigned to mesophase-to-crystal

transition. The sample, sandwiched between two glass covers, was then heated on a hot stage and the changes observed under a polarized optical microscope (POM) were as follows: it melted at about 89 °C and then cleared to an isotropic liquid at 193 °C. On cooling from the isotropic liquid phase, batonetts of smectic A developed at 133 °C, which transformed into the smectic A phase at 126 °C (Fig. 6b). Hence, the complex has liquid crystal properties of a calamitic mesogen. Similar mesophase was found for $[Co(C_{16}\text{-terpy})_2](BF_4)_2$ compound[33].

For compound **2**, its DSC (Fig. 5b) shows three endotherms on heating at 56.4 °C (ΔH = +11.7 kJ mol^{-1}) assigned to H-bonds breaking involving coordinated water, at 85.3 °C (ΔH = +64.2 kJ mol^{-1}) assigned to crystal-crystal transititon and 176.8 °C (ΔH = +55.6 kJ mol^{-1}) assigned to crystal-to-mesophase transition. On cooling from 250 °C, three exotherms formed at 166.4 °C (ΔH = -31.8 kJ mol^{-1}), 57.6 °C (ΔH = -21.9 kJ mol^{-1}) and 40.6 °C (ÄH = -28.6 kJ mol^{-1}), all of which cannot be assigned with certainty. The sample, observed under POM, was found to darken at about 83 °C and then melted at about 175 °C. On cooling from 250 °C, an optical texture was observed at 209 °C (Fig. 6c).

For compound **3**, its DSC (Fig. 5c) shows two overlapping endotherms on heating at 77 °C ($\Delta H_{combined}$ = -48 kJ mol^{-1}), assigned to crystal-to-crystal and crystal-to-isotropic liquid transitions (the latter was observed at 104 °C under POM). Its DSC shows no peaks on cooling from 180 °C to room temperature and POM did not show any optical textures. Hence, it may be concluded that 3 was not mesogenic.

Conclusion

$[Fe(L1)_2](BF_4)$ (**1**), $[Fe_2(OOC(CH_2)_{14}CH_3)_2(L2)\ (H_2O)_2]$ (**2**) and $[Fe_2(OOC(CH_2)_{14}CH_3)_2(L3)(H_2O)_4]\cdot 2.5\ H_2O$ (**3**) were new Fe(II) complexes of three structurally different Schiff bases. These complexes were thermally stable ($T_{dec} > 200$ °C) and except for compound **2**, has melting temperatures lower than 100 °C. Complex **1** has one low-spin Fe(II) atom, low optical band gap (1.8 eV) and exhibited enantiotropic SmA mesomorphism. Complex **2** has two high-spin Fe(II) atoms, low optical bandgap (1.9 eV) and exhibited mesomorphism (s). Complex **3** also has two high-spin Fe(II) atoms at room

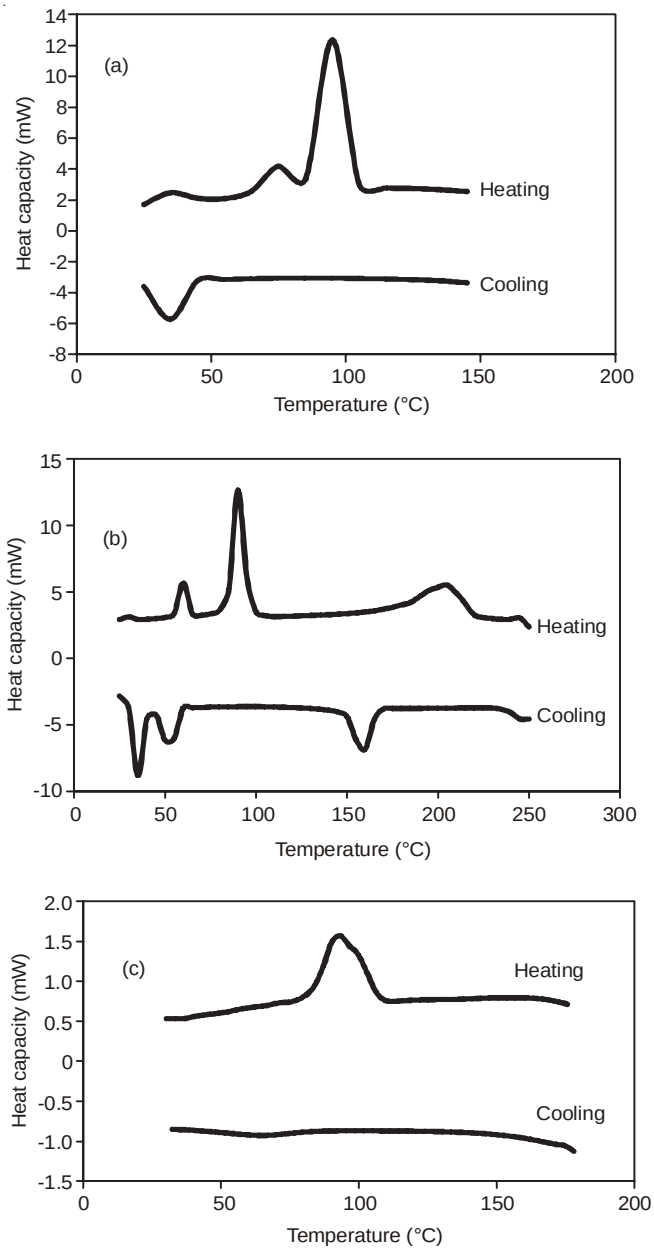

Fig. 5. DSC scans for one heating-cooling cycle of: compound **1** (a); compound **2** (b); and compound **3** (c)

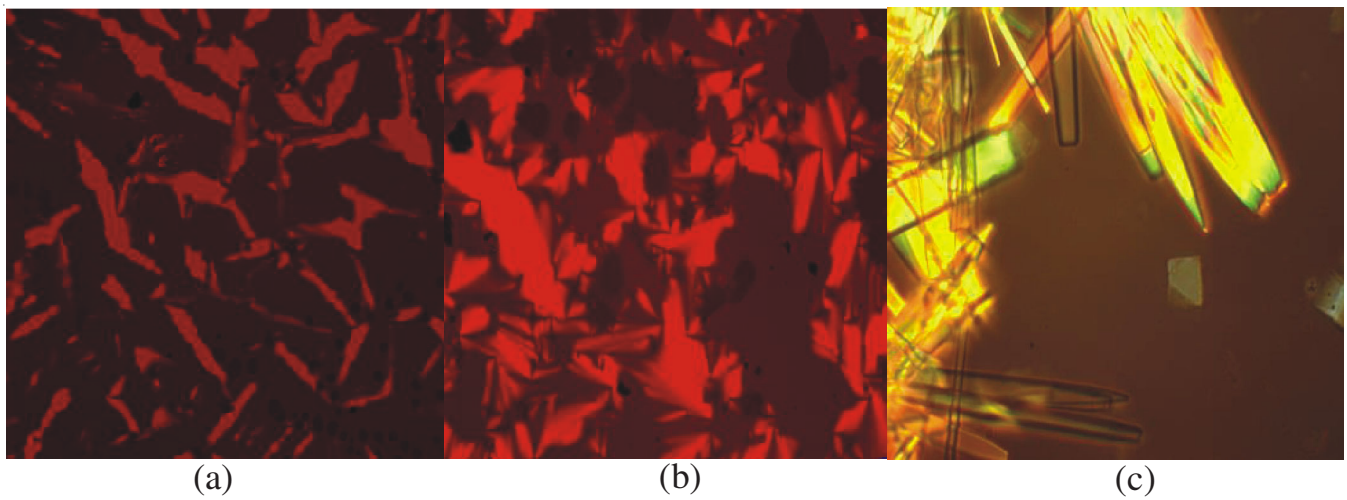

Fig. 6. Photomicrographs of: compound **1** on cooling from the isotropic liquid phase at 133 °C (a) and 126 °C (b); and compound **2** on cooling at 209 °C

temperature with weak antiferromagnetic interaction and incomplete SCO at low temperature, large optical bandgap (2.3 eV), but no liquid crystal properties. Hence, these complexes are potential SCO materials, but only compound **1** is a potential dye-sensitized solar cell material.

ACKNOWLEDGEMENTS

The authors acknowledge the Malaysia Ministry of Education for High Impact Research Grant (UM.C/625/1/HIR/MOHE/05) and University of Malaya for postgraduate research grants (PV056-2012A and PG023-2013A). Thanks are also due to Prof. Malcolm A. Halcrow, School of Chemistry, University of Leeds, Leeds, United Kingdom for useful suggestions and Prof. Takayoshi Kuroda-Sowa, Department of Chemistry, Faculty of Science and Engineering Kinki University, Osaka, Japan for providing the use of Quantum Design MPMS XL EverCool SQUID magnetometer.

REFERENCES

1. P. Gütlich and H.A. Goodwin, Spin Crossover in Transition Metal Compounds, In: Topics in Current Chemistry, Springer, Berlin-Heidelberg, pp. 233-235 (2004).
2. A. Abedi, V. Amani, R. Bocá, L. Dlhán, H.R. Khavasi and N. Safari, *Inorg. Chim. Acta*, **395**, 58 (2013).
3. C. Atmani, F. El Hajj, S. Benmansour, M. Marchivie, S. Triki, F. Conan, V. Patinec, H. Handel, G. Dupouy and C.J. Gómez-García, *Coord. Chem. Rev*., **254**, 1559 (2010).
4. A.B. Gaspar, M. Seredyuk and P. Gütlich, *J. Mol. Struct*., **924-926**, 9 (2009).
5. Y. Bodenthin, G. Schwarz, Z. Tomkowicz, M. Lommel, Th. Geue, W. Haase, H. Möhwald, U. Pietsch and D.G. Kurth, *Coord. Chem. Rev*., **253**, 2414 (2009).
6. P. Gütlich, *Struct. Bond.*, **44**, 83 (1981).
7. S. Ferrere and B.A. Gregg, *J. Am. Chem. Soc*., **120**, 843 (1998).
8. S. Ferrere, *Chem. Mater*., **12**, 1083 (2000).
9. S. Ferrere, *Inorg. Chim. Acta*, **329**, 79 (2002).
10. S. Günes and N.S. Sariciftci, *Inorg. Chim. Acta*, **361**, 581 (2008).
11. N. Sekar and V.Y. Gehlot, *Resonance*, **15**, 819 (2010).
12. A. Hagfeldt, G. Boschloo, L. Sun, L. Kloo and H. Pettersson, *Chem. Rev*., **110**, 6595 (2010).
13. J. Song, Z. Luo, H. Zhu, Z. Huang, T. Lian, A.L. Kaledin, D.G. Musaev, S. Lense, K.I. Hardcastle and L. Hill, *Inorg. Chim. Acta*, **363**, 4381 (2010).
14. R.M. O'Donnell, P.G. Johansson, M. Abrahamsson and G.J. Meyer, *Inorg. Chem*., **52**, 6839 (2013).
15. P.G. Bomben, K.C.D. Robson, B.D. Koivisto and C.P. Berlinguette, *Coord. Chem. Rev*., **256**, 1438 (2012).
16. V.B. Badwaik, R.D. Deshmukh and A.S. Aswar, *J. Coord. Chem*., **62**, 2037 (2009).
17. Y.-G. Li, D.-H. Shi, H.-L. Zhu, H. Yan and S.W. Ng, *Inorg. Chim. Acta*, **360**, 2881 (2007).
18. P.G. Cozzi, *Chem. Soc. Rev*., **33**, 410 (2004).
19. A.D. Garnovskii, A.L. Nivorozhkin and V.I. Minkin, *Coord. Chem. Rev*., **126**, 1 (1993).
20. A.M. Giroud-Godquin, *Coord. Chem. Rev*., **178-180**, 1485 (1998).
21. G.S. Attard and P.R. Cullum, *Liq. Cryst*., **8**, 299 (1990).
22. S.T. Ha, G.Y. Yeap and P.L. Boey, *Int. J. Phys. Sci*., **5**, 2185 (2010).
23. J. Seo, S.T. Moon, J. Kim, S.S. Lee and K.M. Park, *Bull. Korean Chem. Soc*., **24**, 17 (2003).
24. B.C. Smith, Infrared Spectral Interpretation: A Systematic Approach, CRC Press, United States (1998).
25. G.B. Deacon and R.J. Philips, *Coord. Chem. Rev*., **33**, 227 (1980).
26. A.B.P. Lever, Inorganic Electronic Spectroscopy, Elsevier, Amsterdam, edn 2, p. 437 (1984).
27. C. Huang, Y. Chan, F. Liu, D. Tang, J. Yang, Y. Lai, J. Li and Y. Liu, *J. Mater. Chem*., **1**, 5402 (2013).
28. O. Kahn, Molecular Magnetism, VCH Publishers Inc., New York (1993).
29. J.P. Jesson, S. Trofimenko and D.R. Eaton, *J. Am. Chem. Soc*., **89**, 3158 (1967).
30. G. Sowjanya, N.C.G. Reddy, S.L. Reddy, B.J. Reddy and R.L. Frost, *Spectrochim. Acta A*, **71**, 751 (2008).
31. P. Gütlich, A.B. Gaspar and Y. Garcia, *Beilstein J. Org. Chem*., **9**, 342 (2013).
32. Y. Farina and D.A. Rice, *Pertanika J. Sci. Technol*., **3**, 211 (1995).
33. S. Hayami, Y. Kojima, D. Urakami, K. Ohta and K. Inoue, *Polyhedron*, **28**, 2053 (2009).